Model-based EEG and MEG Source Reconstruction Methods

Michael Wagner, Manfred Fuchs, Hans-Aloys Wischmann,
Ralf Drenckhahn, and Thomas Köhler

Philips GmbH Forschungslaboratorien
Röntgenstr. 24-26, D-22335 Hamburg, Germany
wagner@pfh.research.philips.com

Neurophysiological activity, as measured with EEG or MEG, has its origin in the brain. For most EEG and MEG experiments it is known beforehand, that the folded gray matter of the cortex is the location of the neurons whose activity is measured. These neurons, the pyramidal cells, are oriented perpendicular to the cortical surface. Triangulation of the segmented cortical surface yields a triangle net holding all anatomical information which is necessary to guide the reconstruction procedure. We have developed dedicated 3D region-growing, surface subsampling, normal estimation, and surface triangulation algorithms for generating the cortical triangle net. Especially, triangle nets encode neighborhood information of the potential source locations. Neighborhood information provides additional source constraints that model the correlation of neuronal activation which is necessary to generate detectable fields or potentials at all. In a surface-based 3D visualization environment, reconstruction results are displayed as color-coded overlays together with the cortical surface, the measurement setup, and arbitrary MR data slices. The algorithms described are part of the source reconstruction software package CURRY.

Keywords: EEG, MEG, CURRY, source reconstruction, surface triangulation, cortical constraints

1 Introduction

Electroencephalography (EEG) and magnetoencephalography (MEG) are noninvasive methods to measure the electrical activity of the brain. Previous studies [1] revealed, that all available information should be incorporated in solving the bioelectrical respectively biomagnetical inverse problem. Its ill-posedness, which is due to the large number of possible source configurations and the comparatively small number of sensors, cannot be resolved totally. But there is evidence that it may be reduced by applying constraints which model properties of the underlying neurophysiology, so that meaningful results can be obtained. Examples of successfully imposed constraints are the restriction of the solution space to the cortical surface and the fixation of source orientations to the local cortex normal [2], as well as the limitation of source strengths to neurophysiologically achievable values [3], and the spatial [3,4,5] or temporal [3] coupling of neighbored sources.

If cortical neighborhood can be defined, spatial coupling may be combined with the cortical constraints just mentioned. A prerequisite is the triangulation of the cortical surface. The triangle representation can be used for more than just source reconstruction: it also provides an intuitive way of viewing its results.

2 Methods

2.1 Image processing

The three-dimensional shape of the human cortex is segmented from a T1-weighted 3D MR data set as described in [2]. The segmentation algorithm combines thresholding, erosion, 3D region-growing, dilation, and surface extraction in a single fast procedure.
Support points which densely sample the shape of the cortex are then distributed over the extracted surface. The typical point-to-point or thinning distance is 2-3mm, measured along the segmented surface [2]. This leads to some ten thousand points, which will later become the vertices of the triangle net.

Finally, the 3D Delaunay triangulation of the set of points is computed, and exterior tetrahedra are removed. The hull of the remaining tetrahedra is the triangulated surface. By distributing interior support vertices and explicitly using the discrete (voxel) nature of the underlying data, triangulation may be performed in linear time O(N), with N the number of vertices [6].

The surface normals at the vertices are be estimated by computing and averaging the gray level gradients [7] of all voxels of the surface patch around the vertex with the thinning distance as diameter.

2.2 Volume conductor modeling

The volume conductor model consists of the three compartments skin, skull, and brain. Each compartment is assumed to have homogeneous and isotropic conductivity. The forward calculation of fields resp. potentials is performed using the Boundary Element Method (BEM), for which the compartment borders have to be known. The skin surface and the outside of the skull are represented by 600 triangles each, while 1200 triangles are used for the inside of the skull. Due to an optimized Auto Solid Angle approximation [8], a virtual triangle refinement using the vertex normals, and a weighted Isolated Problem Approach [9], the BEM-induced inverse localization error remains in the order of millimeters throughout the brain.

2.3 Linear estimation approach to source reconstruction

A data term and a model term are minimized simultaneously:

$$\text{Min } \Delta^2(\underline{J}) \quad \text{with} \quad \Delta^2(\underline{J}) = \left\| \underline{\underline{C}} \left(\underline{M} - \underline{\underline{L}}\,\underline{J} \right) \right\|^2 + \lambda \left\| \underline{\underline{B}}\,\underline{\underline{W}}\,\underline{J} \right\|^2 . \tag{1}$$

For m sensors, n source locations and one timepoint, $\underline{M}$ is the m-dimensional vector of measured EEG and MEG data. $\underline{J}$ is the n-dimensional vector of source activity to be reconstructed. For each location, one scalar value represents the dipole moment perpendicular to the cortical surface. $\underline{\underline{L}}$ is the mxn lead field matrix modeling the conducting properties of the human head. $\underline{\underline{C}}$ is the inverse square root of the mxm sensor covariance matrix. λ is the Tikhonov regularization parameter. $\underline{\underline{W}}$ is the diagonal nxn lead field normalization matrix as in [10], and $\underline{\underline{B}}$ is the n-column source model matrix. The solution of equation 1 with respect to the source vector $\underline{J}$ is

$$\underline{\hat{J}} = \left(\underline{\underline{W}}^T \underline{\underline{B}}^T \underline{\underline{B}}\,\underline{\underline{W}}\right)^{-1} \underline{\underline{L}}^T \underline{\underline{C}}^T \left(\underline{\underline{C}}\,\underline{\underline{L}}\left(\underline{\underline{W}}^T \underline{\underline{B}}^T \underline{\underline{B}}\,\underline{\underline{W}}\right)^{-1} \underline{\underline{L}}^T \underline{\underline{C}}^T + \lambda \underline{\underline{1}}\right)^{-1} \underline{\underline{C}}\,\underline{M}\,. \tag{2}$$

As equation 2 involves inverting $\underline{\underline{W}}^T\underline{\underline{B}}^T\underline{\underline{B}}\,\underline{\underline{W}}$, one might instead choose to minimize equation 1 directly. The model matrix $\underline{\underline{B}}$ provides the framework for imposing spatial constraints on the source strengths. For more than one timepoint, $\underline{\underline{B}}$ also holds temporal constraints, coupling source activity at one timepoint to activity at the same location (or at neighbored locations, if a spreading of activity shall be enforced), but one instant later or earlier. For minimum norm least squares [11], $\underline{\underline{B}}$ is the unit matrix.

2.4 Nonlinear optimization approach to source reconstruction

Leaving the field of linear estimation theory, we replace the quadratic model term by a more general one and get

$$\Delta^2(\underline{J}) = \left\|\underline{\underline{C}}\left(\underline{M} - \underline{\underline{L}}\,\underline{J}\right)\right\|^2 + \lambda f\left(\underline{\underline{B}}\,\underline{\underline{W}}\,\underline{J}\right) \quad \text{with} \quad f\left(\underline{X}\right) = \sum_i h(x_i), \tag{3}$$

where $h(x)$ is the model function. For L_1-norm reconstructions, $\underline{\underline{B}}$ is the unit matrix and

$$h(x) = |x|\,. \tag{4}$$

L_1-norm reconstructions have the advantage of avoiding the smearing-effect of the standard minimum L_2-norm approaches, as they account better for the additivity of source strengths with regard to the measured signals. If the L_1-norm or the infinity norm are used for the data term, the simplex method of linear programming may be used for the optimization [12].

For modeling of discontinuities, $\underline{\underline{B}}$ is the gradient or surface laplacian matrix, ξ is a typical source strength and

$$h_\xi(x) = \begin{cases} x^2 & \text{for } |x| < \xi \\ \xi^2 & \text{else} \end{cases}, \tag{5}$$

following the weak membrane approach of Blake and Zisserman [13].

3 Results

For a 3D MR image with 256^3 one-byte voxels, the segmentation of the cortical surface took 7 seconds on a sparcstation 10/51. The segmented cortex consisted of 850.000 voxels, 200.000 of which were located on the surface. The distribution of support points with a thinning or subsampling distance of 3mm took another 5 seconds and resulted in 20.000 points distributed over the cortical surface. The generation of cortical surface triangles took 250 seconds. 40.000 triangles were generated. The computation of surface normals took 3 seconds. Figure 1 shows a slice of the original image and a volume-rendering of the segmented cortex, figure 2 a) shows details of a surface-rendering of the generated triangle net. Figure 2 b) shows the three compartments of a volume conductor model.

a) 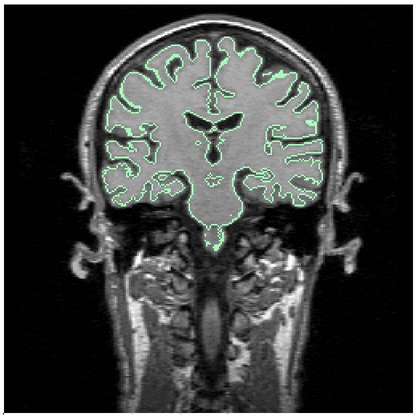

b) 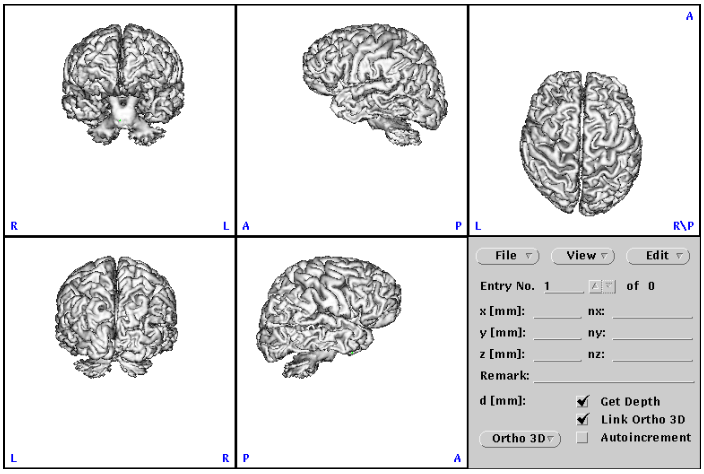

Figure 1: segmentation result a) in a coronal slice b) in five different views

a) 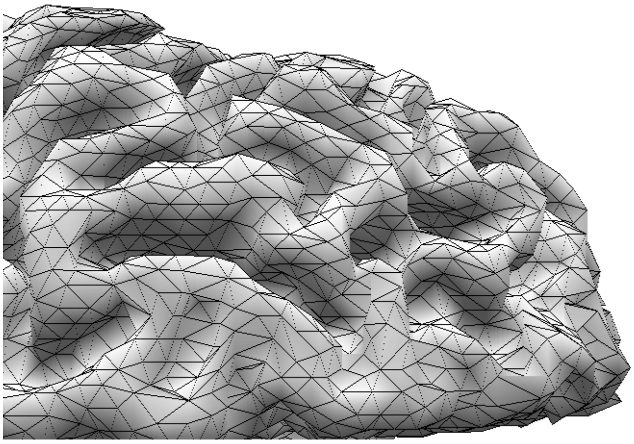

b) 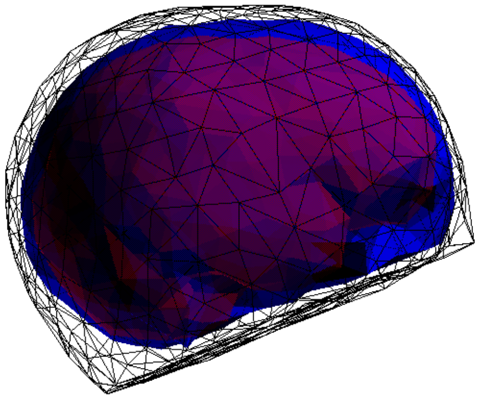

Figure 2: a) cortical triangle net (detail), b) volume conductor model (skin, skull, brain)

The results of the source reconstructions can be visualized as in figure 3: as discrete current dipoles located at the vertices of the cortical triangle net, or as surface-renderings of the triangle nets, shaded according to the reconstructed source strengths. In the 3D scenario shown in figure 4 a), the false color coded results are plotted semi-transparently together with the lighted and shaded anatomical surface. In addition, the segmented and triangulated skin surface, a nearly horizontal slice of the 3D voxel image, the EEG electrodes, and contour lines representing the measured electric potentials are shown. The rendering of the image took 15 seconds without dedicated graphics hardware.

Figures 4 b) and c) show the results of the nonlinear weak membrane reconstruction of a somatosensory evoked field 20ms after stimulus, measured with the Philips 31-channel MEG system [14], signal-to-noise ratio = 10, with and without an additional L_1-norm constraint imposed upon the source strengths for the rejection of silent sources.

Image sequences showing the rotation or the temporal change of a 3D scenario can be viewed as movies. Image pairs from slightly different viewpoints may be used for stereoscopic display.

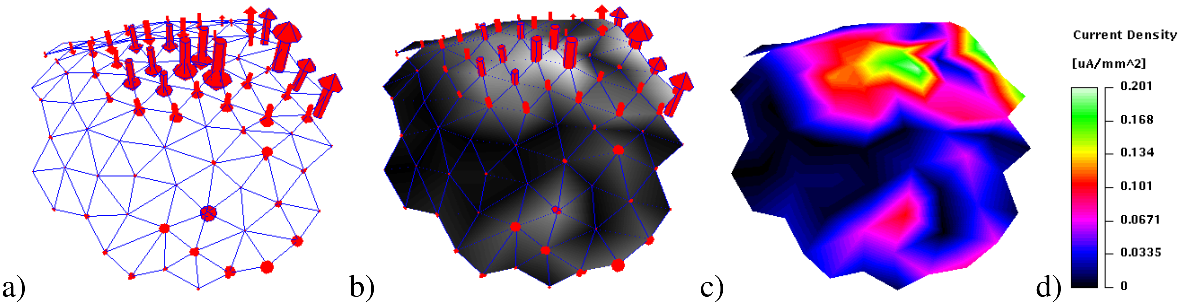

Figure 3: different visualization approaches on a triangle net: a) discrete dipoles b) grayscale intensity shading c) false color shading. The used colorscale is shown in d)

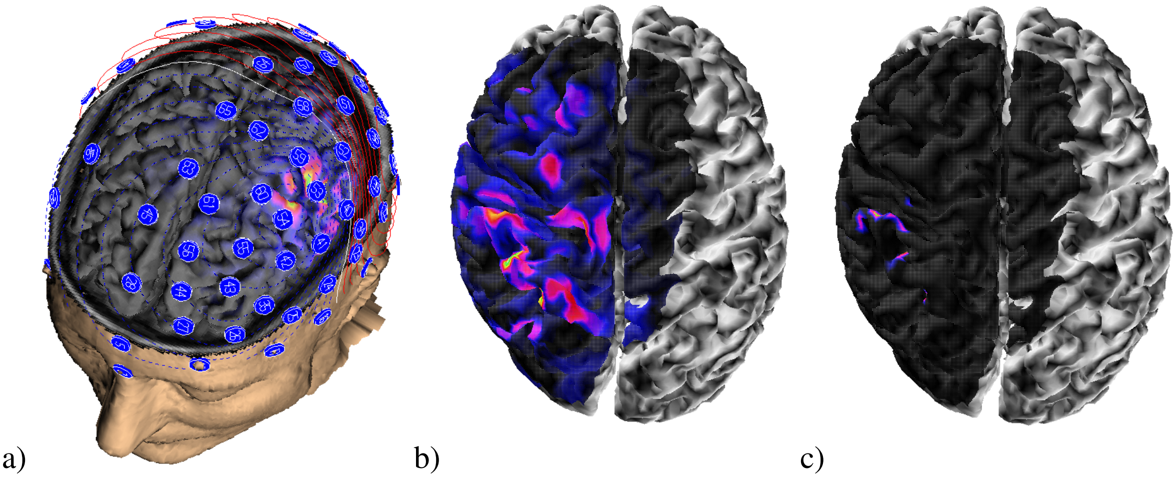

Figure 4: a) overlay of functional (minimum norm) and anatomical data for a somatosensory evoked potential EEG experiment. b) weak membrane reconstruction of evoked field MEG data without and c) with additional L_1-norm constraint. Bright areas denote activated cortex.

4 Discussion

Triangle nets provide a powerful way of encoding anatomical input for source reconstruction algorithms as well as for display routines which render the reconstruction results. All anatomical information that is needed for imposing neurophysiological constraints can be extracted from a triangle net. In particular, these are the possible source locations, the cortical area represented by each location, the local surface normal, and the connections to neighbored locations.

If localization accuracy is critical and/or discontinuous source distributions shall be modeled, the linear estimation approach to source reconstruction cannot be used. Non-quadratic source constraints and dedicated optimization algorithms have to be employed.

References

[1] Fuchs M, Wagner M, Wischmann HA, Ottenberg K, Dössel O: Possibilities of Functional Brain Imaging using a Combination of MEG and MRT, in: Oscillatory Evoked Brain Dynamics, Ed. C. Pantev, Plenum Press, New York, 435-457, 1994

[2] Wagner M, Fuchs M, Wischmann HA, Ottenberg K, Dössel O: Cortex Segmentation from 3D MR images for MEG reconstructions, in: Biomagnetism: Fundamental Research and Clinical Applications, Eds. C. Baumgartner et al, Elsevier/IOS Press, Amsterdam, 433-438, 1995

[3] Wagner M, Fuchs M, Wischmann HA, Drenckhahn R: Weak Membrane Reconstruction of Cortical Current Densities, Proc. ISBET, Münster, 1994, to be published

[4] Pascual-Marqui RD, Michel CM, Lehmannn D: Low Resolution Electromagnetic Tomography: A New Method for Localizing Electrical Activity in the Brain, Int. Journal of Psychophysiology, 18:49-65, 1994

[5] Wagner M, Fuchs M, Wischmann HA, Drenckhahn R, Köhler T: Smooth Reconstruction of Cortical Sources from EEG or MEG Recordings, NeuroImage, 3(3):S168, 1996

[6] Wagner M, Fuchs M, Wischmann HA, Drenckhahn R: Representation of Individual Anatomy by Triangle Nets for Current Reconstruction, Volume Conductor Modeling, and Visualization, in: Mapping Cognition in Time and Space, Eds. H.J. Heinze et al, Birkhaeuser, Boston, 1996, in print

[7] Höhne KH, Bernstein R: Shading 3D-Images from CT using Gray Level Gradients, IEEE Trans. Med. Imaging, 5:45-47, 1988

[8] Wischmann HA, Drenckhahn R, Wagner M, Fuchs M: Systematic Distribution of the Auto Solid Angle and Related Integrals onto the Adjacent Triangles for the Node Based Boundary Element Method, Medical and Biological Engineering and Computing, 34(Supplement 1, Part 2):245-246, 1996

[9] Fuchs M, Drenckhahn R, Wischmann HA, Wagner M: Bioelectric and Biomagnetic Reconstructions with an Improved Boundary Element Method for Realistic Volume Conductor Modeling, IEEE Trans. Biomed. Eng., 1996, submitted

[10] Fuchs M, Wagner M, Wischmann HA: Generalized Minimum Norm Least Squares Reconstruction Algorithms, ISBET Newsletter (ISSN 0947-5133), (5):8-11, 1994

[11] Wang JZ, Williamson SJ, Kaufmann L: Magnetic Source Images Determined by a Lead-Field Analysis: the unique Minimum-Norm Least-Squares Estimation, IEEE Trans. Biomed. Eng., 39:665-675, 1992

[12] Wagner M, Fuchs M, Wischmann HA, Köhler T, Drenckhahn R: Current Density Reconstructions Using the L_1 Norm, in: Proceedings of the BIOMAG 96, Springer, New York, 1996, in print

[13] Blake A, Zisserman A: Visual Reconstruction, MIT Press, Cambridge, 1987

[14] Dössel O, David B, Fuchs M, Krüger J, Lüdeke KM, Wischmann HA: A 31-Channel SQUID System for Biomagnetic Imaging, Applied Superconductivity, 1:1813-1825, 1993